Structurally stable beams in the turbulent atmosphere: dark and antidark beams on incoherent background [Invited]

Zhiheng Xu,[1,2,3] Xin Liu,[1,2] Yangjian Cai,[1,2,5] Sergey A. Ponomarenko,[3,4,*] and Chunhao Liang[1,2,6]

[1]*Shandong Provincial Engineering and Technical Center of Light Manipulation & Shandong Provincial Key Laboratory of Optics and Photonic Devices, School of Physics and Electronics, Shandong Normal University, Jinan 250014, China*
[2]*Collaborative Innovation Center of Light Manipulations and Applications, Shandong Normal University, Jinan 250358, China*
[3]*Department of Electrical and Computer Engineering, Dalhousie University, Halifax, Nova Scotia, B3J 2X4, Canada*
[4]*Department of Physics and Atmospheric Science, Dalhousie University, Halifax, Nova Scotia, B3H 4R2, Canada*
[5]*e-mail: yangjian_cai@163.com*
[6]*e-mail: chunhaoliang@sdnu.edu.cn*
*Corresponding author: serpo@dal.ca

We demonstrate analytically and verify numerically that recently discovered, and experimentally realized, partially coherent dark and antidark beams are structurally stable on propagation in a statistically homogeneous, isotropic random medium, such as the turbulent atmosphere. The dark/antidark beams defy diffraction in free space, and they manifest themselves as dark/bright notches/bumps against an incoherent background. The structure of a bump/notch remains invariant on propagation of the beam through the random medium, while the peak amplitude of the bump/notch decays with the propagation distance in the medium at a rate dependent on the strength of the medium turbulence. We also evaluate numerically the scintillation index of such beams and show that it is significantly lower than that of generic, low-coherence Gaussian Schell-model beams. The combination of structural stability and low scintillations makes partially coherent dark/antidark beams very promising candidates for information transfer and optical communications through atmospheric turbulence.   © 2022 Optica Publishing Group

1. INTRODUCTION

Overcoming the deleterious effects of atmospheric turbulence on the light propagating from a source to a receiver presents one of the most formidable challenges of modern optical communications [1]. In this context, it has been demonstrated not too long ago [2,3] that reducing spatial coherence of the source can mitigate turbulence-induced transverse spatial and angular spreading of light beams generated by such sources. Most of the work in this direction to date, however, has been focused on employing statistically homogeneous light sources, such as a Gaussian Schell-model (GSM) source [4,5]. More recently, the quest for applications of partially coherent light to optical communications has shifted to explore non-uniformly correlated optical sources [6–8]. In particular, it has been demonstrated lately [9] that any member of a certain class of partially coherent vortex fields with a structured cross-spectral density in a closed form derived in [10] is able to maintain its vortex structure in the atmosphere under any turbulence conditions. The separability of the orbital angular momentum of such beams, induced by their vortex structure, from their spatial distribution in the

transverse plane and the robustness of their phase singularities against atmospheric turbulence makes these beams attractive candidates for optical communications.

To our knowledge, however, all the beams, both coherent and partially coherent that have been designed for optical communications applications to date, suffer severe structural degradation due to atmospheric turbulence, especially over long propagation distances or in the strong turbulence regime. One of the most devastating consequences of the interaction of a beam with the turbulence is the loss of a well-defined spatial structure of the beam whereby the average spatial intensity distribution of the source is often dramatically distorted as the beam generated by the source propagates through the turbulence. Yet, distinct features of spatial intensity distributions of structured beams are often utilized for information encoding/decoding in optical communications [11]. In this connection, one may pose a fundamental question: Do there exist structurally stable beams whose intensity distribution is largely immune to fluctuations in the turbulent atmosphere? As most realistic random media, including the practically important case of the turbulent atmosphere, feature statistically

homogeneous, isotropic refractive index fluctuations, we will limit our search for structurally stable beams to this generic class of random media.

To address the just-mentioned fundamental question in this work, we demonstrate analytically and confirm numerically that recently discovered ideal dark or antidark (DAD) beams on incoherent background, which defy free-space diffraction, can be viewed as structurally stable on propagation through any statistically homogeneous and isotropic random medium, such as the turbulent atmosphere. In particular, we show that the profile of the average spatial intensity of any DAD beam remains invariant on propagation through the turbulent atmosphere. The only effect of the medium turbulence is that the peak intensity of a bright bump, or dark notch on an incoherent background, decays on propagation through the turbulence until it ultimately fades into the background. Our results are applicable to the turbulence of any strength with any spectrum of refractive index fluctuations. We verify numerically that structural stability of ideal DAD beams pertains to finite-power apertured DAD beams, which can be realized in the laboratory. We also show numerically that the DAD beam scintillation index (SI) is significantly lower than that of a generic GSM beam, especially in the strong turbulence regime. The combination of structural stability of their average intensity profile and low scintillation footprint makes DAD beams very promising candidates for information transfer and optical communications through the turbulent atmosphere.

This work is organized as follows. In the following section, we present our analytical theory of structural stability of ideal DAD beams in any statistically homogeneous isotropic random medium. In Section 3, we present the results of our numerical simulations to evaluate the average intensity profile and SI of apertured DAD beams. We demonstrate excellent agreement between our analytical results for the average intensity profile of ideal DAD beams and our numerical simulations of the same quantity for apertured DAD beams, which indicates the robustness of the DAD beam structural stability. We draw our conclusions in Section 4.

2. STRUCTURALLY STABLE BEAMS IN TURBULENCE: ANALYTICAL THEORY

Let us start by reviewing key properties of any partially coherent beam consisting of a bright bump or a dark notch against an incoherent background. First of all, we demonstrated in [6] that the cross-spectral density W of any partially coherent diffraction-free beam in free space, which characterizes second-order correlations of the optical fields of the beam at a pair of points $\mathbf{r}_1$ and $\mathbf{r}_2$ in a transverse plane of the beam, is of the form

$$W(\mathbf{r}_1, \mathbf{r}_2) = \Phi(\mathbf{r}) + \Psi(\mathbf{R}), \tag{1}$$

where we introduced the difference and center-of-mass coordinates as

$$\mathbf{r} = \mathbf{r}_1 - \mathbf{r}_2, \quad \mathbf{R} = \frac{(\mathbf{r}_1 + \mathbf{r}_2)}{2}. \tag{2}$$

Notice that the average optical intensity of the beam reads

$$\langle I(\mathbf{r}) \rangle \equiv W(\mathbf{r}, \mathbf{r}) = \Phi(0) + \Psi(\mathbf{r}), \tag{3}$$

where $\Phi(0)$ represents a constant (incoherent) background for the bump/notch of the profile $\Psi(\mathbf{r})$ to ride on.

As a consequence of the Hermiticity of the cross-spectral density, the arbitrary functions Φ and Ψ must obey the following constraints:

$$\Psi^*(\mathbf{R}) = \Psi(\mathbf{R}), \quad \Phi^*(-\mathbf{r}) = \Phi(\mathbf{r}). \tag{4}$$

In addition, the cross-spectral density must be nonnegative definite, which is a nontrivial constraint, in general. One way to satisfy it is to find a series expansion of W in terms of coherent modes with nonnegative coefficients (modal weights). We showed elsewhere [6] how a class of such beams, which we termed dark/antidark diffraction-free beams, can be constructed yielding the cross-spectral density in a closed form,

$$W(\mathbf{r}, \mathbf{R}) \propto J_0(\beta|\mathbf{r}|) + \alpha J_0(\beta|\mathbf{R}|), \tag{5}$$

up to an irrelevant normalization constant. Here $J_0(x)$ is a Bessel function of the first kind and of order zero; β and α are real parameters, with $|\alpha| \leq 1$ to ensure the nonnegative definiteness of the cross-spectral density.

Further, we have shown in [12] that the average intensity distribution of any bump/notch against an incoherent background in a statistically homogeneous, isotropic random medium at a distance z away from the source can be expressed as

$$\langle I(\mathbf{r}, z) \rangle = \Phi(0) + \frac{k^2}{z^2} \int d^2\mathbf{r}' \Psi(\mathbf{r} - \mathbf{r}') \tilde{\Gamma}_m\left(\frac{k|\mathbf{r}'|}{z}, z\right). \tag{6}$$

Here the tilde denotes a Fourier transform, and Γ_m is a two-point medium correlation function of the form [1]

$$\Gamma_m(|\mathbf{r}_1 - \mathbf{r}_2|, z)$$

$$= \exp\left\{-4\pi^2 k^2 z \int_0^1 d\xi \int_0^\infty d\kappa \, \kappa \, S_n(\kappa)[1 - J_0[\kappa(1-\xi)|\mathbf{r}_1 - \mathbf{r}_2|)]]\right\}, \tag{7}$$

where $S_n(\kappa)$ is a spatial spectrum of the refractive index fluctuations.

On substituting from Eq. (5) into Eq. (6), we obtain

$$\langle I(\mathbf{r}, z) \rangle \propto 1 + \frac{\alpha k^2}{z^2} \int d^2\mathbf{r}' J_0\left(\beta|\mathbf{r} - \mathbf{r}'|\right) \tilde{\Gamma}_m\left(\frac{k|\mathbf{r}'|}{z}, z\right). \tag{8}$$

Further, using the summation theorem for Bessel functions [13],

$$J_0(\beta|\mathbf{r} - \mathbf{r}'|) = \sum_{l=-\infty}^{\infty} J_l(\beta r) J_l(\beta r') e^{il(\phi - \phi')}, \tag{9}$$

in Eq. (8) and performing a trivial angular integration, we arrive at

$$\langle I(r, z) \rangle \propto 1 + \alpha I_{\max}(z) J_0(\beta r). \tag{10}$$

Here the peak average intensity of the bump/notch is given by

$$I_{\max}(z) = \frac{2\pi k^2}{z^2} \int_0^\infty dr' r' J_0(\beta r') \tilde{\Gamma}_m\left(\frac{kr'}{z}, z\right), \tag{11}$$

where the Fourier transform of the medium correlation function can be expressed as

$$\tilde{\Gamma}_m\left(\frac{kr'}{z}, z\right) = \int_0^\infty \frac{dx}{2\pi} x J_0\left(\frac{kr'}{z}x\right) \Gamma_m(x, z). \qquad \textbf{(12)}$$

In deriving Eq. (12), we made use of the fact that the medium fluctuations are isotropic and performed the angular integration using the integral representation of the Bessel function [14],

$$J_0\left(\frac{kxr'}{z}\right) = \int_0^{2\pi} \frac{\mathrm{d}\phi}{2\pi} \exp\left(i\frac{kxr'}{z}\cos\phi\right). \qquad \textbf{(13)}$$

Next, we introduce an auxiliary variable $s = kr'/z$ and rewrite Eqs. (11) and (12) as

$$I_{\max}(z) = 2\pi \int_0^\infty ds\, s\, J_0(s\beta z/k)\tilde{\Gamma}_m(s, z), \qquad \textbf{(14)}$$

$$\tilde{\Gamma}_m(s, z) = \int_0^\infty \frac{\mathrm{d}x}{2\pi} x J_0(sx)\Gamma_m(x, z), \qquad \textbf{(15)}$$

respectively. Further on combining Eqs. (14) and (15) and interchanging the order of integration, we arrive at

$$I_{\max}(z) = \int_0^\infty dx\, x\Gamma_m(x, z) \int_0^\infty ds\, s\, J_0(sx)J_0(s\beta z/k). \qquad \textbf{(16)}$$

Finally, using the completeness relation for the Bessel functions [14],

$$\int_0^\infty \mathrm{d}x\, x J_0(\nu x)J_0(\mu x) = \frac{1}{\nu}\delta(\nu - \mu), \qquad \textbf{(17)}$$

and performing a trivial integration with the delta function, we arrive at our final expression for the intensity profile of an ideal structurally stable beam in a random medium in the form

$$\langle I(r, z)\rangle \propto 1 + \alpha\Gamma_m\left(\frac{\beta z}{k}, z\right) J_0(\beta r), \qquad \textbf{(18)}$$

where the medium correlation function is re-expressed as

$$\Gamma_m(\beta z/k, z)$$

$$= \exp\left\{-4\pi^2 k^2 z \int_0^1 \mathrm{d}\xi \int_0^\infty \mathrm{d}\kappa\, \kappa\, S_n(\kappa)\left[1 - J_0\left[\frac{\kappa(1-\xi)\beta z}{k}\right]\right]\right\}. \qquad \textbf{(19)}$$

We can now draw a few noteworthy conclusions:

1. The discovered structurally stable beams maintain their spatial profiles at the expense of having the peak intensities of their bumps/notches diminished on propagation in random media.
2. The peak intensity decay rate, given by Eq. (19), is determined solely by the medium correlation function.
3. Our results depend neither on a type of random medium, nor on the strength of the turbulence in the medium, as long as the turbulence is statistically homogeneous and isotropic.
4. By implication from the previous remark, our results are directly applicable to light propagation through the turbulent atmosphere.

5. Our derivation does not employ the usual quadratic approximation for the medium correlation function in the turbulent atmosphere, which is known to have several caveats [15].

We note that the individual coherent modes, $\{J_m(\beta r)e^{im\phi}\}$, composing each DAD beam at the source, are not invariant in the turbulent medium, although they are diffraction-free in free space. Yet, a judicious superposition of such uncorrelated modes yields a shape-invariant partially coherent beam over a distance determined by the strength of the medium turbulence. Finally, we notice that the presented DAD beams are idealized as they carry infinite power. It is then of great interest to find out whether finite-power realizations of such beams, realized by aperturing each coherent mode, for example, maintain their structural stability in the turbulence. In the next section, we address this crucial issue via numerical simulations.

3. NUMERICAL SIMULATION OF DAD BEAM PROPAGATION THROUGH TURBULENCE

In this section, we first briefly introduce a multiple phase screen (MPS) method for numerical simulation of the DAD beam propagation in a random medium. We will focus on the case of the turbulent atmosphere as the latter has direct practical significance for optical communications. We then compare our numerical results with the corresponding theoretical results of the previous section to affirm the validity of our analytical conclusions beyond the ideal DAD beam approximation. Lastly, we employ the MPS method to study the SI behavior of DAD beams in the turbulent atmosphere.

A. Introduction to the Multiple Phase Screen Method

The evolution of a beam in the turbulent atmosphere is determined by the interplay of free-space diffraction and atmospheric turbulence. Within the framework of the MPS method, the propagation distance z is divided into N segments of equal length $\Delta z = z/N$. We assume that, inside each segment of length Δz [see Fig. 1(a)], the atmospheric turbulence effects play out within a very thin layer [see Fig. 1(b)], which we replace by a phase screen with desired turbulence statistics. Hence, the cumulative evolution of the beam in the turbulent atmosphere
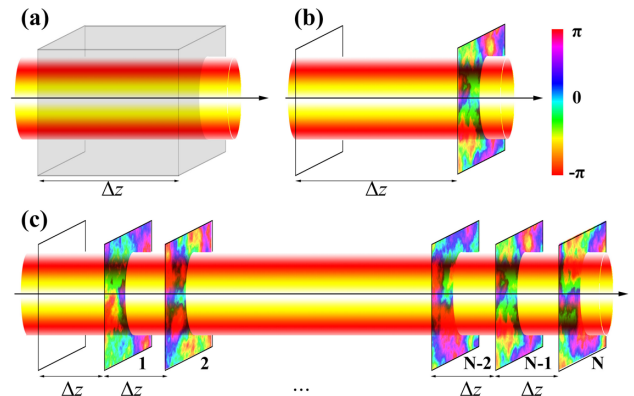

Fig. 1. Schematics for the multiple phase screen technique to numerically study beam propagation in the turbulent atmosphere.

consists of a sequence of alternating free-space propagation segments of length Δz and phase screens. In greater detail, the MPS method works as follows. First, we assume that all phase screens are "frozen." Each mode of a given ensemble realization of a DAD beam propagates sequentially through all phase screens as indicated in Fig. 1(c). We then superpose all the propagated modes, composing the DAD ensemble realization in question, at a receiving plane. Thus, we can quantitatively describe the evolution of the given DAD ensemble realization through the turbulent atmosphere. Next, we "refresh" all phase screens to ensure another DAD ensemble realization "sees" a different statistical realization of the atmosphere, and we redo all the above operations for the next realization. As a result, we amass a database of statistical realizations of DAD beams, which have propagated over a given stretch of the turbulent atmosphere, that enables us to infer the average intensity distribution as well as statistics (SI) of DAD beams in the turbulent atmosphere [16–19]. In essence, the implementation of the MPS is conceptually similar to that of a split-step Fourier approach of nonlinear fiber optics [20].

We can now write

$$U_z = T_N \times H_N\{\dots T_k \times H_k\{\dots T_1 \times H_1\{U_0\}\}\}, \quad k \in [2, N-1],$$ (20)

where U_0 and U_z are the electric fields of the beam in the source and receiver planes, respectively. $H_k\{\}$ is a free-space transfer function in the kth segment, and $T_k = \exp(i\psi_k)$ is a transmission function of the corresponding random phase screen. Further, ψ_k is an accumulated phase induced by the turbulence over the distance Δz. It is given by

$$\psi_k = \text{Re}\{F_T\{C_k \times \Phi_\theta\}\},$$ (21)

where Re and F_T stand for the real part of a complex number and a Fourier transform, respectively. Next, C_k is a circular complex Gaussian random function. We refresh C_k to refresh the phase screens. $\Phi_\theta = 2\pi \Delta z k^2 \Phi_n$ characterizes the power spectrum of the phase screen with Φ_n being the power spectrum of refractive index fluctuations. To describe the latter quantitatively, we adopt the modified von Karman spectrum, given by [1]

$$\Phi_n(\kappa) = 0.033 C_n^2 \frac{\exp\left(-\kappa^2/\kappa_m^2\right)}{\left(\kappa^2 + \kappa_0^2\right)^{11/6}}, \quad 0 \le \kappa < \infty,$$ (22)

with $\kappa_m = 5.92/l_0$ and $\kappa_o = 2\pi/L_0$. Here C_n^2 is a so-called structure constant characterizing the strength of refractive index fluctuations; l_0 and L_0 denote the inner and outer scales of the turbulence, respectively. In the following numerical simulations, we assume $l_0 = 1$ mm and $L_0 = 1$ m.

B. Numerical Simulation Results and Comparison with Analytical Theory

The cross-spectral density of a DAD beam field at the source has a coherent mode representation as [6,8]

$$W(\mathbf{r}_1, \mathbf{r}_2) = \sum_{m=-M}^{m=M} \lambda_m \psi_m^*(\mathbf{r}_1, z) \psi_m(\mathbf{r}_2, z).$$ (23)

Here the coherent modes $\{\psi_m\}$ read

$$\psi_m(\mathbf{r}) = J_m(\beta r) \exp(im\phi),$$ (24)

and the modal weights are specified by $\lambda_m = 1 + (-1)^m \alpha$, $|\alpha| \le 1$. In theory, the number of coherent modes required to reproduce an ideal DAD beam is infinite. However, a reliable representation of finite-power DAD beams can be realized in the laboratory with a finite (large) number of modes [8]. In practice, each coherent mode needs to be truncated to ensure it carries a finite amount of power. To this end, we use a circular function of radius r_0 to truncate each mode according to the following rule:

$$\psi_m^A(\mathbf{r}) = \psi_m(\mathbf{r}) circ(\mathbf{r}/r_0),$$ (25)

where

$$circ(\mathbf{r}/r_0) = \begin{cases} 1, & |\mathbf{r}| \le r_0; \\ 0, & \text{otherwise.} \end{cases}$$ (26)

Having truncated all modes, we can study the evolution of DAD beams in the turbulent atmosphere with the aid of the MPS method. In the following, we will present our simulation results. The parameters of the source and the medium are as follows: $M = 21$, $r_0 = 1$ m, $\beta = 3.625 \times 10^{-5} k$, and $k = 2\pi/\lambda$ corresponding to the wavelength $\lambda = 632.8$ nm. The distances Δz between adjacent phase screens are adopted to be 30 m, 60 m, 200 m, 500 m, and 667 m for $C_n^2 = 10^{-13}$m$^{-2/3}$, 10^{-14} m$^{-2/3}$, 10^{-15} m$^{-2/3}$, 10^{-16} m$^{-2/3}$, and 10^{-17} m$^{-2/3}$, respectively. They meet the Rytov coefficient requirements [16,17].

First, we explore the intensity evolution of DAD beams during propagation. It follows from Eq. (18) that the intensity profile of an ideal DAD beam remains invariant and the turbulence only affects its peak intensity. To compare numerical results for truncated beams with theoretical predictions for ideal DAD beams concisely yet comprehensively, we exhibit in Fig. 2 the on-axis intensity of DAD beams as a function of the propagation distance for different C_n^2. The theoretical results, obtained from Eq. (18), are displayed with solid curves. We can infer from the figure that, for any DAD beam, ideal or apertured, the on-axis intensity $I(0, z)$ gradually increases/decreases to unity, which is the incoherent background intensity (in arbitrary units). It follows that any bump/notch gradually disappears due to the atmospheric turbulence until it completely fades into the background over a certain critical distance. Clearly, the usefulness of DAD beams for optical communications is limited by the critical distance, which, in turn, depends on the turbulence strength. As is anticipated, the lower C_n^2, the lower the rate at which a structural feature (bump or notch) vanishes. We display our simulation results with the solid curves with triangles as seen in Fig. 2. The up-pointing and down-pointing triangles correspond to antidark and dark beams, respectively. We can conclude by comparing our numerical results with our analytics that the two are in excellent agreement for any strength of the turbulence. We can then conclude that structural stability in the turbulence is not limited to ideal DAD beams but is well translated to finite-power DAD beams.

Next, we examine the SI of DAD beams propagating in the turbulent atmosphere. The SI, employed to quantify the strength of intensity fluctuations of light, is defined as [18]

$$\sigma^2(\mathbf{r}) = \langle I^2(\mathbf{r})\rangle / \langle I(\mathbf{r})\rangle^2 - 1,$$ (27)
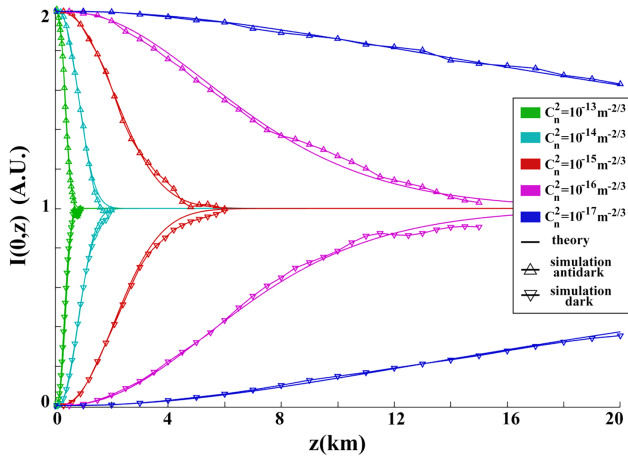
Fig. 2. On-axis intensity $I(0, z)$ of DAD beams propagating in the turbulent atmosphere. Our color scheme is explained in the inset. Our theoretical results are exhibited with solid curves. Our numerical results for antidark beams ($\alpha = 1$) and dark beams ($\alpha = -1$) are displayed with solid curves with up-pointing triangles and down-pointing triangles, respectively. The number of phase screens is $N = 30$.

where the angle brackets denote ensemble averaging.

In Fig. 3, we show the average intensity and SI evolution of the DAD beam propagating in the weakly turbulent atmosphere. The structure constant is chosen as $C_n^2 = 1 \times 10^{-16}$ m$^{-2/3}$. To highlight the effect of immunity to the turbulence, we compared the SI of a DAD beam with that

of a conventional GSM beam. The cross-spectral density of the latter reads [5]

$$W(\mathbf{r}_1, \mathbf{r}_2) \propto \exp\left(-\frac{\mathbf{r}_1^2 + \mathbf{r}_2^2}{4\delta_I^2}\right)\exp\left[-\frac{(\mathbf{r}_1 - \mathbf{r}_2)^2}{2\delta_c^2}\right], \quad \textbf{(28)}$$

where δ_I and δ_c denote the rms beam width and transverse coherence width at the source, respectively. To simulate GSM beam propagation through the turbulent atmosphere with the MPS method, we first employ a complex screen method to generate a statistical ensemble of a GSM source [21]. We then follow the same MPS steps as those we took to study DAD beam propagation through the atmosphere to evaluate statistical properties of GSM beams. To furnish a fair comparison, we stipulate that the GSM beam width be the same as that of the DAD beam's central bump/notch. To this end, we employ the following definition of the beam width s [22]

$$s^2 = \frac{\int d\mathbf{r} r^2 \langle I(\mathbf{r})\rangle}{\int d\mathbf{r}\langle I(\mathbf{r})\rangle}. \quad \textbf{(29)}$$

A straightforward calculation yields the rms width of 75 mm for a DAD beam bump/notch. Hence, in the following numerical simulations, we adopt $\delta_I = 75$ mm and $\delta_c = 25$ mm for a GSM beam. It is by now firmly established that partially coherent beams with lower coherence are better able to resist turbulence-induced degradation than their more coherent cousins [16]. In this connection, a GSM beam with $\delta_c^2/\delta_I^2 \ll 1$ can be treated as nearly incoherent. In Fig. 3(a), we display the density plots of the average intensity and SI distributions for
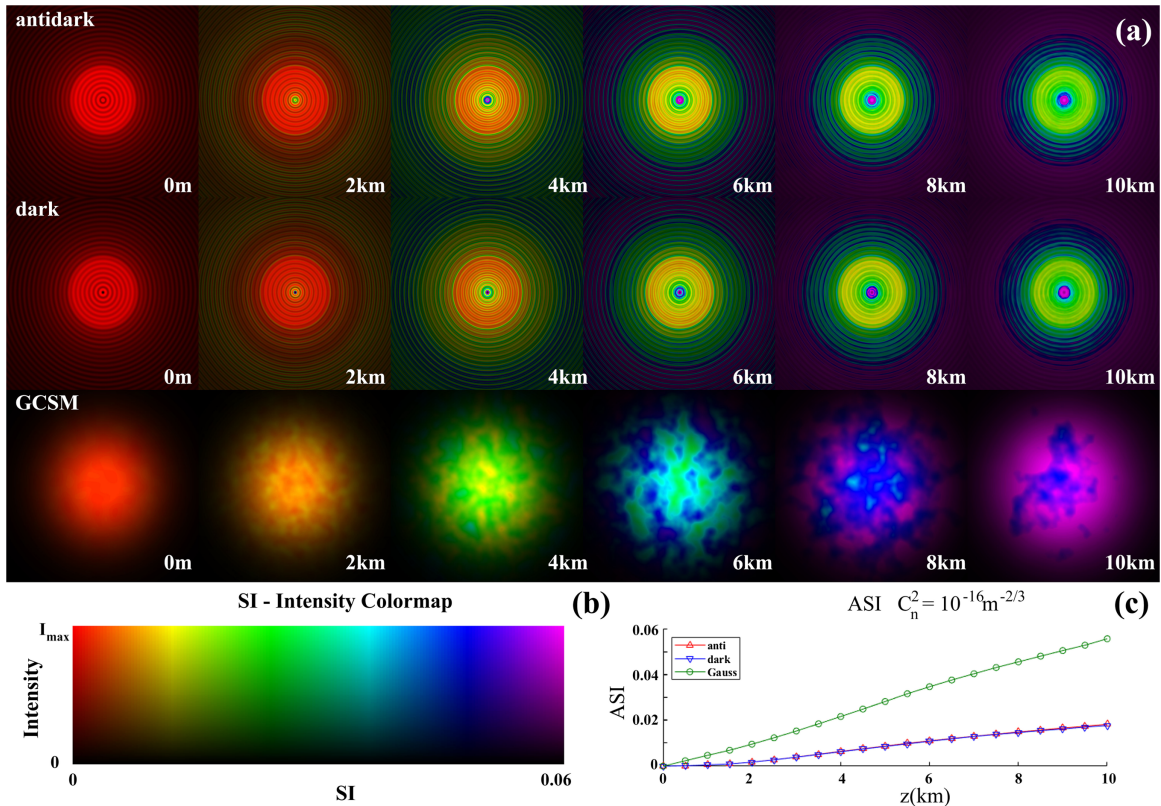

Fig. 3. (a) Density plots of the SI and intensity of the DAD and GSM beams propagating in the turbulent atmosphere. (b) SI-intensity colormap. Its hue and brightness describe the scintillation index and intensity, respectively. (c) Plots of the ASIs of the DAD and GSM beams versus the propagation distance. The parameters are chosen as $C_n^2 = 1 \times 10^{-16}$ m$^{-2/3}$ and $N = 20$.

DAD and GSM beams with the just-described parameters propagating in the turbulent atmosphere. We adopt an SI-Intensity colormap, shown in Fig. 3(b). The hue and brightness of the map quantify the SI and average intensity, respectively. We find that, in the weak turbulence, $C_n^2 = 1 \times 10^{-16}$ m$^{-2/3}$, the average intensity profiles of the antidark beam (top row) and dark beam (middle row) remain almost invariant with the propagation distance over distances up to $z = 10$ km. However, the density plot colors change from red at $z = 0$ km to green at $z = 10$ km, implying that the SI notably increases with the propagation distance for both beams. We observe though that, at the same propagation distance, the colors of the density plots of dark and antidark beams are the same. We can then infer that both types of beams display qualitatively the same behavior in the turbulent atmosphere. At the same time, we notice that the density plot color of a GSM beam, whose behavior is exhibited in the bottom row, changes from red at $z = 0$ km to purple at $z = 10$ km. We then conclude that even low source coherence GSM beams are much more prone to succumbing to the turbulence than are DAD beams. To reaffirm this point, we plot an average SI (ASI) over a transverse cross section of each beam versus the propagation distance. ASI is defined as ASI $= \frac{1}{D} \int_D \sigma^2(\mathbf{r}) d\mathbf{r}$. D is given by a circular area of radius 75 mm in our numerical simulations. The relevant result is exhibited in Fig. 3(c). The ASI curves of all beams monotonically increase with the propagation distance. As anticipated above, the red and blue curves, corresponding to the antidark and dark beams, respectively, completely overlap. Further, the ASI curve of a GSM beam grows faster than the ones for DAD

beams. As an example, at $z = 10$ km, the ASIs for the GSM and DAD beams are 0.056 and 0.018, respectively.

Next, we explore the average intensity evolution and scintillations of DAD beams in the atmosphere with stronger turbulence. The structure constant is then chosen as $C_n^2 = 1 \times 10^{-13}$ m$^{-2/3}$. All evolution scenarios are qualitatively similar to those considered above in the weak turbulence regime. However, as we observe in Fig. 4, ASIs are 0.38 and 0.12 for a GSM beam and DAD beam, respectively, at a fairly short propagation distance, $z = 450$ m. That is, GSM beam scintillations are more than 3 times those of a DAD beam. Undoubtedly, the difference in scintillation behavior of GSM and DAD beams will only grow with the propagation distance. Therefore, we have shown that DAD beams have superior characteristics in the turbulent atmosphere compared to any garden variety, i.e., GSM partially coherent beam. The superiority of DAD beams is especially noticeable when the turbulence is stronger.

4. CONCLUSION

We have explored the structural stability of optical beams on propagation through the turbulent atmosphere. We have demonstrated analytically that a recently discovered class of DAD partially coherent beams, which are diffraction-free in free space, remain structurally stable on propagation through a statistically homogeneous isotropic random medium, such as the turbulent atmosphere. In particular, each DAD diffraction-free beam is characterized by a bright bump or a dark notch against an incoherent background. We have shown that DAD beams maintain their structure of a bright bump/dark notch
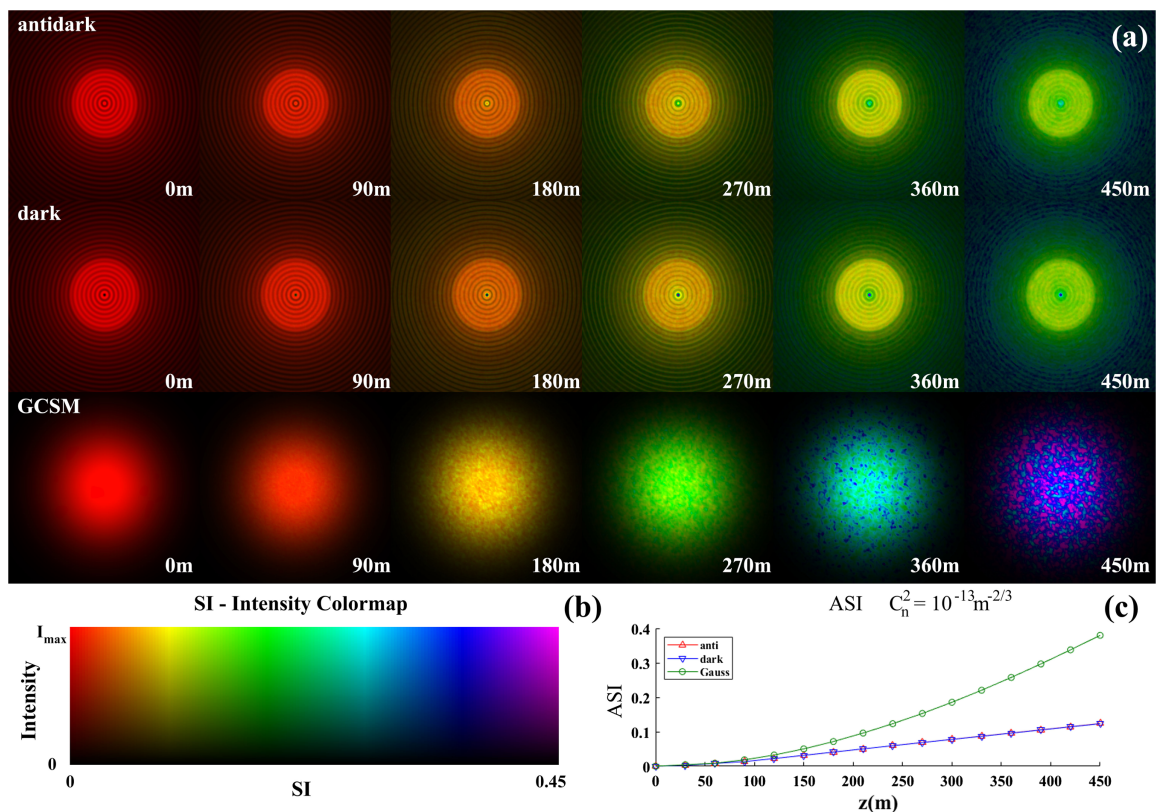

Fig. 4. Same quantities as those in Fig. 3. The parameters are chosen as $C_n^2 = 1 \times 10^{-13}$ m$^{-2/3}$ and $N = 15$.

against an incoherent background in the turbulent atmosphere. Moreover, the spatial profile of the bump/notch is maintained as well. The turbulence, however, causes the peak intensity of the bump/notch to decay on propagation at the rate dependent on the turbulence strength. Our analytical results pertain to ideal, infinite-power DAD beams. We have compared our analytics with numerical simulations for the propagation of finite-power realizations of DAD beams and found excellent agreement between the two. We have also numerically investigated the SI of DAD beams and compared its behavior with that of low-coherence GSM beams. We found that DAD beams have much lower scintillations than low-coherence GSM beams under any turbulence conditions. The superiority of DAD beams is especially pronounced in the strong turbulence situation. The combination of structural stability and low SI makes DAD beams promising candidates for optical communications, optical trapping, and laser radar applications, among others.

Disclosures. The authors declare no conflicts of interest.

Data availability. Data underlying the results presented in this paper are not publicly available at this time but maybe obtained from the authors upon reasonable request.

REFERENCES

1. L. C. Andrews and R. L. Phillips, *Laser Beam Propagation in Turbulent Atmosphere*, 2nd ed. (SPIE, 2005).
2. S. A. Ponomarenko, J.-J. Greffet, and E. Wolf, "The diffusion of partially coherent beams in turbulent media," Opt. Commun. **208**, 1–8 (2002).
3. G. Gbur and E. Wolf, "Spreading of partially coherent beams in random media," J. Opt. Soc. Am. A **19**, 1592–1598 (2002).
4. G. Gbur, "Partially coherent beam propagation in atmospheric turbulence," J. Opt. Soc. Am. A **31**, 2038–2045 (2014).
5. L. Mandel and E. Wolf, *Optical Coherence and Quantum Optics* (Cambridge University, 1995).
6. S. A. Ponomarenko, W. Huang, and M. Cada, "Dark and anti-dark diffraction-free beams," Opt. Lett. **32**, 2508–2510 (2007).
7. H. Lajunen and T. Saastamoinen, "Propagation characteristics of partially coherent beams with spatially varying correlations," Opt. Lett. **36**, 4104–4106 (2011).
8. X. Zhu, F. Wang, C. Zhao, Y. Cai, and S. A. Ponomarenko, "Experimental realization of dark and antidark diffraction-free beams," Opt. Lett. **44**, 2260–2263 (2019).
9. J. Li, X. Chen, S. McDuffie, M. A. M. Najjar, S. M. H. Rafsanjani, and O. Korotkova, "Mitigation of atmospheric turbulence with random carrying OAM," Opt. Commun. **446**, 178–185 (2019).
10. S. A. Ponomarenko, "A class of partially coherent beams carrying optical vortices," J. Opt. Soc. Am. A **18**, 150–156 (2001).
11. A. Forbes, M. de Oliveira, and M. R. Dennis, "Structured light," Nat. Photonics **15**, 253–262 (2021).
12. X. Li, S. A. Ponomarenko, Z. Xu, F. Wang, Y. Cai, and C. Liang, "Universal self-similar asymptotic behavior of optical bump spreading in random medium atop incoherent background," Opt. Lett. **45**, 698–701 (2020).
13. I. S. Gradstein and I. M. Ryzhik, *Tables of Integrals, Series, and Products* (Academic, 1980).
14. G. B. Arfken, H. J. Weber, and F. E. Harris, *Mathematical Methods for Physicists* (Academic, 2012).
15. S. M. Wandzura, "Meaning of quadratic structure functions," J. Opt. Soc. Am. **70**, 745–747 (1980).
16. F. Wang, X. Liu, and Y. Cai, "Propagation of partially coherent beam in turbulent atmosphere: a review (invited review)," Prog. Electromagn. Res. **150**, 123–143 (2015).
17. J. D. Schmidt, *Numerical Simulation of Optical Wave Propagation: With Examples in MATLAB* (SPIE, 2010).
18. J. Yu, Y. Huang, F. Wang, X. Liu, G. Gbur, and Y. Cai, "Scintillation properties of a partially coherent vector beam with vortex phase in turbulent atmosphere," Opt. Express **27**, 26676–26688 (2019).
19. F. Wang, J. Yu, X. Liu, and Y. Cai, "Research progress of partially coherent beams propagation in turbulent atmosphere," Acta Phys. Sinica **67**, 18–31 (2018).
20. G. P. Agrawal, *Nonlinear Fiber Optics*, 4th ed. (Academic, 2007).
21. P. Ma, B. Kacerovská, R. Khosravi, C. Liang, J. Zeng, X. Peng, C. Mi, Y. E. Monfared, Y. Zhang, F. Wang, and Y. Cai, "Numerical approach for studying the evolution of the degrees of coherence of partially coherent beams propagation through an ABCD optical system," Appl. Sci. **9**, 2084–2094 (2019).
22. L. Xin, Z. Li, Y. E. Monfared, C. Liang, F. Wang, B. J. Hoenders, Y. Cai, and P. Ma, "Flexible autofocusing properties of ring Pearcey beams by means of a cross phase," Opt. Lett. **46**, 70–73 (2021).